

A new chaotic image encryption algorithm based on transversals in a Latin square

Honglian Shen^{a,b}, Xiuling Shan^{a,*}, Zihong Tian^a

^a*School of Mathematical Sciences, Hebei Normal University, Shijiazhuang, 050024, China*

^b*Department of Mathematics and Computer Science, Hengshui College, Hengshui, 053000, China*

Abstract

There are some good combinatorial structures suitable for image encryption. In this study, a new chaotic image encryption algorithm based on transversals in a Latin square is proposed. By means of an n -transversal of a Latin square, we can permute an image data group by group for the first time, then use two Latin squares for auxiliary diffusion on the basis of a chaotic sequence, finally make use of a pair of orthogonal Latin squares to do the second scrambling. As a whole, the encryption process of “scrambling-diffusion-scrambling” is formed. The experimental results indicate that this algorithm achieves a secure and fast encryption effect. The final information entropy is very close to 8, and the correlation coefficient is approximate to 0. All these tests verify the robustness and practicability of this proposed algorithm.

Keywords: Image encryption, Chaotic, Latin square, Transversals

1. Introduction

In these years, the network communication develops very rapidly, a large amount of public or private image information is transferred via the public internet. How to transmit a lot of image information safely and efficiently has become an increasingly important issue. Image encryption is the main solution. Digital image encryption is a new branch of computer cryptography, and also a relatively independent branch and a research hot issue in the field of information security. Unlike ordinary text information, digital image has a great deal of data, a strong correlation between pixels and other particularities, which makes DES, IDEA and RSA these traditional methods are not appropriate for them [1]. Therefore, various image encryption algorithms have been put forward in the last few years.

In general, an encryption technology involves two aspects: scrambling and diffusion. Scrambling is mainly used to change the pixels' position, while diffusion is used to change the pixels' value.

Chaos-based encryption algorithms play an important role in existing image encryption algorithms [2–7]. Some qualities of a chaotic systems like sensitivity

to initial values, parameter sensitivity, ergodicity, etc. make it particularly appropriate to do image encryption. Meanwhile chaotic systems also have some disadvantages, such as being defined on a set of real numbers, accompanied by short period phenomena, local linearity and uneven distribution, and requiring discretization when used [8], therefore it's easy to be damaged by chosen plaintext attacks or known plaintext attacks. In addition, many algorithms often use high-dimensional chaotic systems[9–13], increasing the complexity and unpredictability. The higher the dimension of the system, the more computations are required. Hence, many new different techniques have been used in image encryption algorithms, including one-time keys [14], bit-level permutation [15–18], DNA coding [19–22], genetic manipulation [23–26], semi-tensor product theory [27, 28], Fractal sorting matrix [29], compressive sensing [7, 30, 31], and combinatorial designs [11–13, 18, 32–35].

Recently, many combinatorial design structures have been applied in cryptography, such as Latin square [12, 32–37], Latin cube [11, 13, 18], Hadamard matrix [38], etc. Using simple chaotic system and these uniform combinatorial design structure as auxiliary, better encryption effect can also be achieved. As early as 1949, Shannon pointed out that a perfect password can be expressed by a Latin square in his classic paper [39]. Kong

*Corresponding author.

Email address: xiulingshan@sina.com (Xiuling Shan)

used Latin squares to build algebraic models for different password systems [40]. A Latin square defined on a finite integer set S is a square matrix, and get uniformity for the same number of occurrences of each element in S , and the total number of Latin squares is also very large. These characteristics of Latin square are very suitable for image encryption, so some algorithms according to Latin square were put forward. In 2001, Li first proposed a method to do the image scrambling using a pair of orthogonal Latin squares [36], which can directly generate a two-dimensional mapping, instantly increasing the scrambling efficiency. However, he didn't give the algorithm of generating orthogonal Latin squares, nor did he do simulation experiments. In 2014, Wu et al. proposed an image encryption scheme by using Latin square [32]. Firstly a Latin square was used to generate a one-dimensional mapping for the scrambling process. Then the Latin square was used to perform bitxor operation on image pixels. However, the scrambling efficiency of this algorithm is low and it is vulnerable to attack. Other algorithms that use Latin squares have the same problem. In 2018, Xu et al. generated a self-orthogonal Latin square (SOLS) and proposed a new algorithm for image encryption [34]. Using a SOLS and its transpose, a pair of orthogonal Latin squares are formed, and the SOLS can provide a pseudo-random sequence for the diffusion process. The experimental results show that this algorithm is safe and highly efficient. The entropy value of encrypted Lena reached 7.997, and the correlation coefficient was small. In 2019, Xu et al. put forward a new image encryption scheme by using 3D bit matrix and orthogonal Latin cubes [18]. Each original image was decomposed into a three-dimensional bit matrix, and a pair of orthogonal Latin cubes were used not only for confusion but also for diffusion, which proved that the algorithm is highly safe and efficient. In 2020, Zhou et al. combined 3D orthogonal Latin squares (3D-OLSs) with matching matrix for color image encryption [13]. The same as algorithm in [18], it fully utilized the orthogonality of 3D Latin cube. In 2021, Zhang et al. proposed an encryption algorithm based on Latin square and random shift [12]. Wang et al. also put forward an image encryption algorithm based on Latin square array [35], utilizing the orthogonality and uniformity of Latin square. In 2021, Hua et al. designed a new CIEA using orthogonal Latin squares and 2D-LSM for color image encryption, realized point-to-point permutation and the random distribution of the pixels in the plain image [11].

As can be seen from the above discussions, better encryption can also be achieved by using the orthogonality and uniformity of Latin squares, together with

other innovations. In addition, there are some other properties of Latin squares that can be utilized, such as transversals. For a Latin square of order n , there exists plenty of n -transversals. By means of an n -transversal, we can divide all n^2 positions into n mutually disjoint groups. So in this article we proposed a novel chaos-based image encryption algorithm according to transversals in a Latin square. Firstly we use a n -transversal to permute the image data group by group in the first round of substitution. We can also define two new Latin squares according to the n -transversal, which can be used for auxiliary diffusion on the basis of a chaotic sequence and achieve a good diffusion effect. Finally a pair of orthogonal Latin squares are reused for the second scrambling. As a whole, the structure of "scrambling-diffusion-scrambling" is formed. Simulation results show that a secure and fast encryption effect is achieved in this algorithm.

In the rest of this article, some primary definitions and conclusions are introduced in Section 2. Section 3 is mainly used to introducing the detailed procedure of encryption and decryption. In Section 4, the experimental results and analysis are demonstrated. In the end, we summarize this article.

2. Preliminaries

2.1. Latin squares and transversals

A Latin square of order n (defined on an n -set S) is an $n \times n$ array in which each cell contains a single symbol, such that each symbol occurs exactly once in each row and column [34]. For consistency, we set $S = \{0, 1, \dots, n-1\}$.

Two Latin squares of order n $A = (a_{ij})$ and $B = (b_{ij})$ are orthogonal if every ordered pair (a_{ij}, b_{ij}) in $S \times S$ occurs exactly once.

Fig. 1 lists a pair of orthogonal Latin squares of order 4 $A = (a_{ij})$ and $B = (b_{ij})$. Denote $C = (c_{ij})$ as the juxtaposition array, where $c_{ij} = (a_{ij}, b_{ij})$. Each ordered pair in $S \times S$ occurs exactly once.

Notation: Using a pair of orthogonal Latin squares $A = (a_{ij})$ and $B = (b_{ij})$ can directly generate a two-dimensional map $\phi : (i, j) \rightarrow (a_{ij}, b_{ij})$, $i, j = 0, 1, \dots, n-1$.

Suppose M is a Latin square defined on S . A transversal in M is a set of n positions, no two in the same row or column, including each of the n symbols exactly once. Two transversals are disjoint if there are no same positions in them. Any k disjoint transversals are called a k -transversal. If $k = n$ there exists an n -transversal in M .

$$A = \begin{pmatrix} 0 & 1 & 2 & 3 \\ 1 & 0 & 3 & 2 \\ 2 & 3 & 0 & 1 \\ 3 & 2 & 1 & 0 \end{pmatrix} \quad B = \begin{pmatrix} 0 & 1 & 2 & 3 \\ 2 & 3 & 0 & 1 \\ 3 & 2 & 1 & 0 \\ 1 & 0 & 3 & 2 \end{pmatrix}$$

$$C = \begin{pmatrix} (0,0) & (1,1) & (2,2) & (3,3) \\ (1,2) & (0,3) & (3,0) & (2,1) \\ (2,3) & (3,2) & (0,1) & (1,0) \\ (3,1) & (2,0) & (1,3) & (0,2) \end{pmatrix}$$

Figure 1: Latin squares A , B and the juxtaposition array C

In Fig. 1, C is the juxtaposition array of A and B . Treat each column of C as a position element set of A . There are 4 positions in the first column, all row numbers and column numbers are different, and the four elements at the four positions of A are 0, 3, 1, 2 respectively, so the first column of C is a transversal of A . The other columns of C are similar. All the positions of A are divided into four pairwise disjoint groups, so there is a 4-transversal in A .

For an additive group G , a bijection θ of G is called a complete mapping if the mapping $\sigma : x \rightarrow x + \theta(x)$ is also a bijection of G [41].

Theorem 1. [42] *The Cayley table M of the additive group $G = \{g_0, g_1, \dots, g_{n-1}\}$ is a Latin square with (i, j) th entry $g_i + g_j$. For a bijection $\theta : G \rightarrow G$, M_θ is the Latin square with (i, j) th entry $g_i + \theta(g_j)$, and the cells $\{(g_i, \theta(g_i)) \mid i = 0, 1, \dots, n-1\}$ form a transversal of M if and only if θ is a complete mapping of G .*

Theorem 2. *Let $F = \{g_0, g_1, \dots, g_{n-1}\}$ be a finite field with character p . M is the Cayley table of F . Let $a \in F$, $a \neq 0, 1$, and $a \not\equiv -1 \pmod{p}$. Define a mapping $\gamma_j : x \rightarrow ax + g_j$ ($j = 0, 1, \dots, n-1$). Then the following conclusions hold.*

- 1) *These γ_j s ($j = 0, 1, \dots, n-1$) are n different complete mappings over F under addition;*
- 2) *Define an $n \times n$ array M_γ with (i, j) th entry $\gamma_j(g_i) = ag_i + g_j$. Then M_γ is a Latin square on F ;*
- 3) *Define $D = (d_{ij})$ with $d_{ij} = (g_i, \gamma_j(g_i))$. All columns of D form n disjoint transversals of M (named D as the truncated decomposition array). Define the array M_1 with (i, j) th entry $g_i + \gamma_j(g_i)$. Then M, M_1, M_γ are pairwise orthogonal Latin squares.*

Appendix A shows the proof of Theorem 2. According to Theorem 2, there are n disjoint transversals in M , where the i th column index in j th transversal is the (i, j) th element of M_γ .

Example 1. Let F be a finite field of order 4. Suppose the primitive polynomial is $\omega^2 + \omega + 1$, where ω is a primitive root of F . Let $F = \{g_0, g_1, g_2, g_3\}$ with $g_0 = 0$, $g_1 = 1$, $g_2 = \omega$, $g_3 = \omega + 1$.

Firstly define the Cayley table M of the field F under addition with (i, j) th entry $g_i + g_j$,

$$M = \begin{pmatrix} 0 & 1 & \omega & \omega + 1 \\ 1 & 0 & \omega + 1 & \omega \\ \omega & \omega + 1 & 0 & 1 \\ \omega + 1 & \omega & 1 & 0 \end{pmatrix}.$$

Let $a = \omega$. Construct another Latin square M_γ with (i, j) th entry $\gamma_j(g_i) = ag_i + g_j$,

$$M_\gamma = \begin{pmatrix} 0 & 1 & \omega & \omega + 1 \\ \omega & \omega + 1 & 0 & 1 \\ \omega + 1 & \omega & 1 & 0 \\ 1 & 0 & \omega + 1 & \omega \end{pmatrix}.$$

Construct the truncated decomposition array D with (i, j) th entry $(g_i, \gamma_j(g_i))$,

$$D = \begin{pmatrix} (0,0) & (0,1) & (0,\omega) & (0,\omega+1) \\ (1,\omega) & (1,\omega+1) & (1,0) & (1,1) \\ (\omega,\omega+1) & (\omega,\omega) & (\omega,1) & (\omega,0) \\ (\omega+1,1) & (\omega+1,0) & (\omega+1,\omega+1) & (\omega+1,\omega) \end{pmatrix}.$$

The four positions of each column of D form a transversal of M , and the set of all columns is a 4-transversal of M .

Finally define the array M_1 with (i, j) th entry $g_i + \gamma_j(g_i) = (1+a)g_i + g_j$,

$$M_1 = \begin{pmatrix} 0 & 1 & \omega & \omega + 1 \\ \omega + 1 & \omega & 1 & 0 \\ 1 & 0 & \omega + 1 & \omega \\ \omega & \omega + 1 & 0 & 1 \end{pmatrix}.$$

According to Theorem 2, M, M_1, M_γ are pairwise orthogonal Latin squares.

2.2. Logistic map

In this article, we adopt the classical Logistic map to generate two new sequences. One of them is used to generate a finite field, and the other is used to do diffusion. We describe Logistic map as follows.

$$x_{i+1} = \lambda x_i(1 - x_i), \quad i = 0, 1, 2, \dots \quad (1)$$

where λ is a system parameter, $0 < \lambda \leq 4$, and $x_i \in (0, 1)$. When $\lambda > 3.573815$, the sequence shows chaos.

3. The proposed image encryption algorithm

For simplicity, some of the symbols are described as follows. n stands for a prime power. Q is used to represent an $n \times n$ original plaintext image, K is the encryption key and *Cipher* denotes the corresponding ciphertext. This algorithm is divided into two parts: Algorithm 1 generates three Latin squares and an n -transversal by use of K and the features of Q ; Algorithm 2 is mainly used for encryption, including three layers: scrambling, diffusion and scrambling, then the encrypted image *Cipher* is formed. The encryption diagram is listed in Fig. 2.

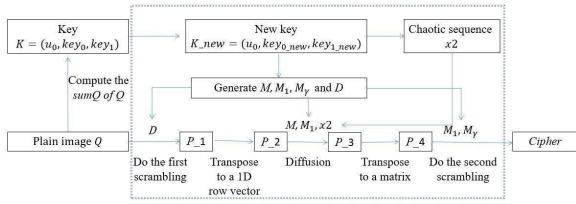


Figure 2: The encryption process

3.1. The generation of Latin squares M, M_1, M_γ and an n -transversal

We use Algorithm 1 to construct three Latin squares and an n -transversal, all of which are directly generated on a finite field, using addition and multiplication in the finite field.

Algorithm 1: The generation of M, M_1, M_γ and an n -transversal

Input: An $n \times n$ plain image Q , encryption key $K = (\mu_0, key_0, key_1)$, public parameter a .

Output: Latin squares M, M_1, M_γ and the truncated decomposition array D .

Step 1: Compute the sum of all pixels in Q , denoted as $sumQ$. Let

$$s = \text{floor}(sumQ/255 \times 10^{15})/10^{15}, \quad (2)$$

where floor is the downward integer function. Compute $key_{0_new} = (key_0 + s)/2$, $key_{1_new} = (key_1 + s)/2$. It's very essential because $sumQ$ reflects the characteristics of the plaintext image. When the plaintext image changes a little, the chaotic sequence will change greatly because of the changed key. In other words, only one round of encryption is needed to achieve a high sensitivity to the plaintext image.

Step 2: Generate a logistic sequence of length n $x_1 = \{x_i \mid i = 0, 1, 2, \dots, n-1\}$ with system parameter μ_0 and initial value $x_0 = key_{0_new}$. Sort x_1 as follows:

$$[fx, lx] = \text{sort}(x_1) \quad (3)$$

where sort is the function that sorts a sequence in ascending order. fx is the new sequence reordered by x_1 , lx is the index position.

Step 3: Redefine operations of addition and multiplication on lx , then generate a finite field F_n with character p . Denote $F_n = \{g_0, g_1, \dots, g_{n-1}\}$. Select $a \in F_n$, $a \neq 0, 1$, and $a \not\equiv -1 \pmod{p}$, generate three Latin squares M, M_1, M_γ with (i, j) th entry $g_i + g_j$, $(1+a)g_i + g_j$ and $ag_i + g_j$ respectively. According to Theorem 2, M, M_1, M_γ are pairwise orthogonal.

Step 4: Generate the truncated decomposition array D with (i, j) th entry $(g_i, ag_i + g_j)$. Then the column set of D is an n -transversal of M .

3.2. Image encryption

We use Algorithm 2 to complete the rest of the encryption process. First of all, with the help of the truncated decomposition array D , we can permute the image data Q group by group. Secondly, we use two Latin squares M and M_1 for auxiliary diffusion based on another chaotic sequence x_2 . Finally, a pair of orthogonal Latin squares M_1 and M_γ are used for the second scrambling. The following is the detailed procedure of Algorithm 2.

Algorithm 2: The proposed encryption algorithm

Input: An $n \times n$ plain image Q , encryption key $K = (\mu_0, key_0, key_1)$, public parameters a, c_1 and c_2 .

Output: Ciphertext image *Cipher*.

Step 1: Make use of Algorithm 1, Q, K and a to generate M, M_1, M_γ and D .

Step 2: Scramble Q for the first time. At first convert D to a natural column index array D_θ by bijection $\theta : g_i \rightarrow i$. Starting from the first transversal, the first pixel of Q at $D_\theta(0, 0)$ is placed at the position $D_\theta(1, 0)$, the second pixel at the position $D_\theta(2, 0)$ is placed at the position $D_\theta(3, 0)$, and so on..., until the last pixel at the position $D_\theta(n-1, 0)$ is placed at the position $D_\theta(0, 0)$. After scrambling n times based on n transversals, we can get a temporary image $P.1$. The specific process is shown below.

$$\begin{cases} P.1(D_\theta(i+1, j)) = Q(D_\theta(i, j)), \\ P.1(D_\theta(0, j)) = Q(D_\theta(n-1, j)), \\ 0 \leq i \leq n-2, \quad 0 \leq j \leq n-1. \end{cases} \quad (4)$$

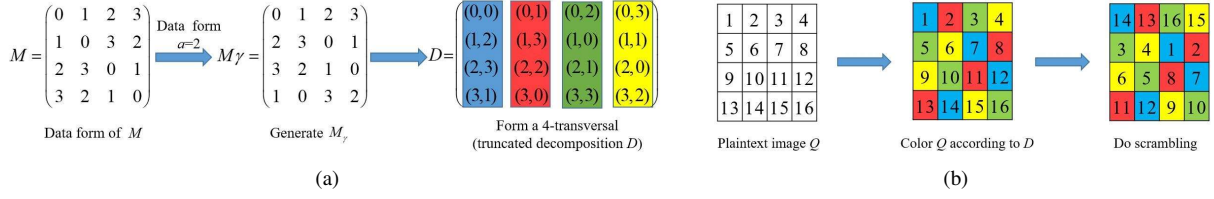


Figure 3: An example of doing scrambling according to a 4-transversal

Fig. 3 shows a 4-order example to illustrate the scrambling process in this step. In Fig. 3(a), A Latin square M (Generated on the field of Example 1) is converted to digital form. Select a number $a = 2$, then generate M_γ with the (i, j) th entry $(1 + a)g_i + g_j$, resulting in a 4-transversal D , all the 16 positions of a 4-order matrix are divided into four pairwise disjoint groups. Because $g_i = i$, $D_\theta = D$, we can scramble Q according to D . In Fig. 3(b), starting from the first transversal, the first pixel 1 at $(0,0)$ is placed at $(1,2)$, the second pixel 7 at $(1,2)$ is placed at $(2,3)$, the third pixel 12 at $(2,3)$ is placed at $(3,1)$, finally, the fourth pixel 14 at $(3,1)$ is placed at $(0,0)$. So are the scramblings of the other transversals. Because D is a 4-transversal, the first scrambling can be completed after 4 times.

Step 3: Firstly convert P_1 into a row vector P_2 , then generate another new chaotic sequence of length $n^2 + 100$ with system parameter μ_0 and initial value key_{1_new} . To eliminate the effect of the initial value, especially delete the first 100 digits, the rest form a new chaotic sequence x_2 . M and M_1 are transposed into row vectors L_M and L_{M1} , which are used as two pseudo-random sequences for auxiliary diffusion to form a new row vector $\{P_3(i)\}_{i=0}^{n^2-1}$. The detailed diffusion formula is as follows.

$$\begin{cases} b = \text{mod}(\text{floor}(x_2(i) * (10^3 + c_1 * L_M(i) \\ + c_2 * L_{M1}(i))), 256), \\ P_3(i) = P_2(i) \oplus b \oplus P_3(i-1). \end{cases} \quad (5)$$

where the initial value $P_3(-1) = 0$, b is a temporary variable, and mod is the module integer function.

Step 4: Transpose P_3 to an array P_4 . By using the orthogonality of M_1 and M_γ , we conduct the second scrambling by formula (6), the final ciphertext image *Cipher* is obtained.

$$\begin{cases} P_4(M_1(i, j), M_\gamma(i, j)) \rightarrow \text{Cipher}(i, j), \\ 0 \leq i, j \leq n-1. \end{cases} \quad (6)$$

3.3. Image decryption

When we do image decryption, follow the reverse procedure, and we need to know the value $\text{sum}Q$ in ad-

vance. The following figure is the decryption diagram.

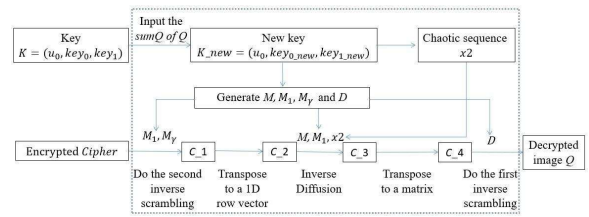


Figure 4: The decryption process

4. Simulation results and security analysis

We conducted simulation experiments and listed all the results in this section. In order to reflect the advantages of this algorithm, we compared this algorithm with some representative algorithms [4, 12, 34, 35, 43–45].

In our experiments, a total of six different 256×256 images are selected for testing, which are chosen from the USC-SIPI2 and CVG-UGR3 image sets. Every experiment requires only one round of encryption, the secret key K is: $\mu_0 = 3.99999$, $key_0 = 0.123456$, $key_1 = 0.234567$. There are three public parameters $a = \omega$ (ω is a primitive root of F_n), $c_1 = 1.3$, $c_2 = 1.5$.

The algorithm was tested from the following aspects: key space and sensitivity analysis, histogram test, correlation test, information entropy test, differential attack resistance test, robustness test, computational complexity and time efficiency analysis, and so on.

4.1. Key space and sensitivity analysis

4.1.1. Key space analysis

There are three real numbers in $K = (\mu_0, key_0, key_1)$, and the computational accuracy of each value is 10^{-15} , so this algorithm can achieve a key space of $10^{45} \approx 2^{149}$, greater than 2^{128} [46–48]. There are also three public parameters to select, so the algorithm has a large enough key space and occupies a relatively small

memory space. In summary, it can resist brute-force attacks.

4.1.2. Key sensitivity analysis

An excellent image encryption algorithm desires strong sensitivity to the key, so sensitivity analysis is often considered as a crucial indicator of resistance to brute-force attacks. It's usually evaluated from two aspects: sensitivity during encryption and sensitivity during decryption.

(1) Key sensitivity analysis during encryption

Take Lena for example. Firstly, set $K = (3.99999, 0.123456, 0.234567)$, then modify each value slightly by adding 10^{-15} after the decimal point. We use two sets of secret keys to encrypt Lena, *Cipher1* being the image encrypted with K and *Cipher2* being the image encrypted with the modified K . Fig. 5 shows the comparison of the results of the two ciphertext images. Percentages of different pixels are computed as shown in Table 1, which are all greater than 99.59%, fully indicating that the algorithm is extremely sensitive to the key during encryption.

Table 1: Key sensitivity test results during encryption

The comparison ciphers	Fig. 5(a)	Fig. 5(b)	Fig. 5(c)
Number of different pixels	65270	65276	65288
percentage	99.5941%	99.6033%	99.6216%

(2) Key sensitivity analysis during decryption

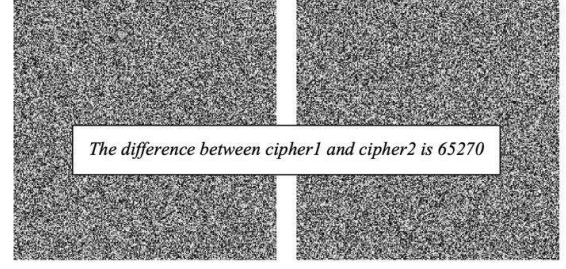
Similarly, Lena is also used to do key sensitivity analysis during decryption. In view of the encrypted image *Cipher*, make a tiny change value 10^{-15} in each value of $K = (3.99999, 0.123456, 0.234567)$, then use the two sets of secret keys to decrypt *Cipher*. Fig. 6 presents when we use the right key, we can obtain the original image, while using the modified key, we can't decrypt correctly. In addition, Table 2 records the percentages of different pixels of two deciphers, all greater than 99.5%. From these results, we can discover that even though the key changes a little, we will fail to obtain the original image. So this algorithm is key-sensitive during decryption.

Table 2: Key sensitivity test results during decryption

Original and decrypted image	Fig. 6(a)	Fig. 6(b)	Fig. 6(c)
Number of different pixels	65274	65290	65227
percentage	99.6002%	99.6246%	99.5285%

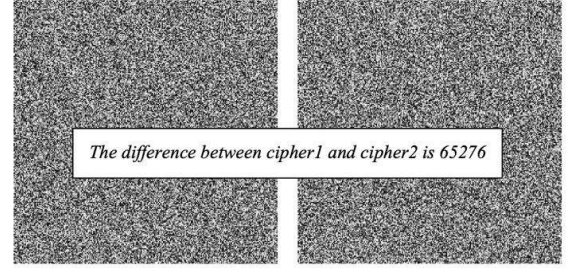
4.2. Statistical Analysis

A good algorithm for image encryption should be capable of resisting any statistical attacks. The main statistical indicators include histogram analysis, correlation



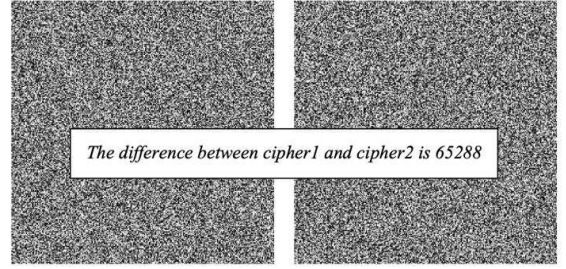
$K = (3.99999, 0.123456, 0.234567)$ $K = (3.99999 + 10^{-15}, 0.123456, 0.234567)$

(a) Two ciphers with μ_0 changed 10^{-15}



$K = (3.99999, 0.123456, 0.234567)$ $K = (3.99999, 0.123456 + 10^{-15}, 0.234567)$

(b) Two ciphers with key_0 changed 10^{-15}



$K = (3.99999, 0.123456, 0.234567)$ $K = (3.99999, 0.123456, 0.234567 + 10^{-15})$

(c) Two ciphers with key_1 changed 10^{-15}

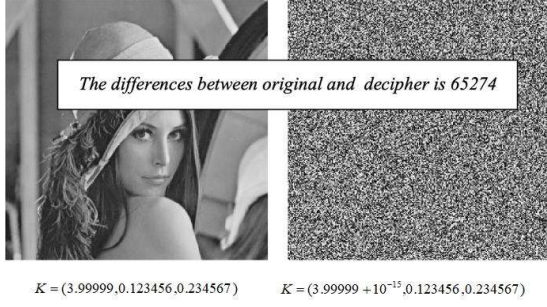
Figure 5: Comparisons of encryption results with key changed

coefficients of adjacent pixels (usually considering three directions) and information entropy analysis.

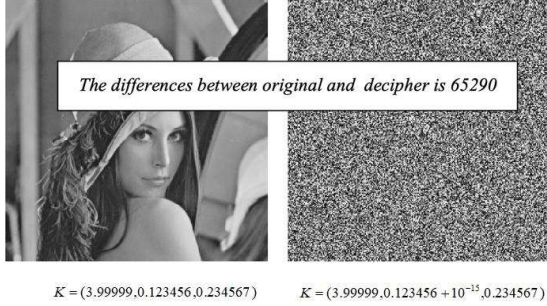
4.2.1. Histogram analysis

In an image, histogram is a representation of the frequency of each gray level pixel. A well-encrypted image has a histogram distribution that is as uniform as possible. In general, it can be measured by variance S , and the formula is as follows:

$$S = \frac{1}{256} \sum_{i=0}^{255} (hist_i - aver)^2. \quad (7)$$



(a) Two deciphers with μ_0 changed 10^{-15}



(b) Two deciphers with key_0 changed 10^{-15}



(c) Two deciphers with key_1 changed 10^{-15}

Figure 6: Comparisons of decryption results with key changed

where $hist_i$ denotes the frequency of the i th gray level pixel, $aver = \frac{1}{256} \sum_{i=0}^{255} hist_i$. S represents the variance of histogram. The smaller the value of S , the better.

Table 3 shows the histogram values of six images before and after encryption, and Fig. 7 shows the histogram distribution of six images before and after encryption. From the data and the figure, we can find that all the histograms of ciphertext images tend to be evenly distributed, and after encryption Lena's variance is as low as 195.766, indicating that this algorithm can effectively resist histogram analysis.

Table 3: The variance of six images

Image	Plaintext	Ciphertext
Lena	41398.1016	195.7656
Baboo	46866.8281	238.9062
Cameraman	105604.8672	227.3594
Clock	282061.5625	205.8984
Couple	86692.7031	252
Man	37058.7812	234.7734

4.2.2. Correlation test

In a plaintext image, there exist strong correlations among adjacent pixels. To resist statistical analysis, correlation in ciphertext images should be as small as possible [49]. We randomly select 4000 pairs of neighbouring pixels, including three directions (horizontal, vertical, and diagonal) to measure the correlations. The required calculation formula is listed in (8):

$$r_{uv} = \frac{cov(u, v)}{\sqrt{D(u)} \sqrt{D(v)}}. \quad (8)$$

where

$$\begin{cases} cov(u, v) = \frac{1}{N} \sum_{i=1}^N (u_i - E(u))(v_i - E(v)) \\ D(u) = \frac{1}{N} \sum_{i=1}^N (u_i - E(u))^2 \\ E(u) = \frac{1}{N} \sum_{i=1}^N u_i \end{cases} \quad (9)$$

where u and v represent the grayscale values of two neighbouring pixels in the image.

To visualize the distribution of images before and after encryption, Fig. 4.2.2 displays the correlation distributions of six different images in three directions. Observing the original image we can note that the neighbouring dots are mainly distributed around the diagonal, while in an encrypted image the dots are evenly distributed throughout the whole plane. That is, the plaintext images are highly correlated in any direction, but the correlations after encryption are very low. Using the calculation formula in Ref. [34], we compute the correlation coefficients of six images before and after encryption, present the results in Table 4. We can see that before encryption the values are very large, but after encryption all numerical results are very small, approximate to 0. For comparison with other algorithms, Table 5 lists the comparison results in the case of Lena. Although the value of Lena in this article is inferior to Refs. [43], it is better than other six Refs [4, 12, 34, 35, 44, 45]. The accuracy of the decimal point is 10^{-3} , which implies that this algorithm achieves a good confusion effect and has strong applicability.

Table 4: Correlation test results of six images in this article

Image	Testing direction			Average value
	Horizontal	Vertical	Diagonal	
Lena	0.94034	0.97136	0.92288	0.94486
Ciphertext image of Lena	-0.00064	-0.00356	-0.00157	0.00192
Baboo	0.78885	0.74049	0.68020	0.73651
Ciphertext image of Baboo	-0.00291	-0.00005	0.00402	0.00233
Cameraman	0.96099	0.97463	0.92712	0.95425
Ciphertext image of Cameraman	0.00198	0.00045	0.00202	0.00148
Clock	0.95009	0.97750	0.93230	0.95330
Ciphertext image of Clock	0.00135	0.00365	-0.00194	0.00231
Couple	0.87446	0.88660	0.80207	0.85438
Ciphertext image of Couple	-0.00067	-0.00159	-0.00023	0.00083
Man	0.93943	0.95108	0.91287	0.93446
Ciphertext image of Man	0.00347	-0.00098	-0.00128	0.00191

4.2.3. Information entropy analysis

An important measure of testing randomness is information entropy, usually denoted as H , which can be measured according to the following formula (10):

$$H(m) = - \sum_{i=0}^{l-1} p(m_i) \log_2 p(m_i). \quad (10)$$

where m_i is the gray value, and there are l kinds of gray values in an image. $p(m_i)$ represents the probability of m_i , and $\sum_{i=0}^{l-1} p(m_i) = 1$. Generally, an image has 256 gray values. Only when the frequency of each gray level is the same, information entropy H reaches the theoretical ideal value 8 [50].

We use the formula (10) to calculate the entropy values of six images before and after encryption, then list the results in Table 6. From the table we can see all values are very close to 8, which shows a good encryption effect. Especially, the information entropy of Lena reaches 7.99784, strong uncertainty of this algorithm has been indicated. Table 5 lists Lena's entropy values in different algorithms. Our results are superior to the other six contrast algorithms. Therefore, the ciphertext images have strong uncertainty and our algorithm can resist entropy attacks.

4.3. Differential attack analysis

A good algorithm can resist differential analysis, requiring different plaintext images (even if with only one different pixel) corresponding to significantly different ciphertext images. In general, there are two commonly used criteria for testing resistance to differential attacks, NPCR and UACI. Let $C_1 = (C_{i,j}^1)$ and $C_2 = (C_{i,j}^2)$ denote two ciphertext images of size $M \times N$, where their plaintext image has only one different pixel. Define binary sequence to the images C_1 and C_2 :

$$D_{i,j} = \begin{cases} 0, & C_{i,j}^1 = C_{i,j}^2 \\ 1, & C_{i,j}^1 \neq C_{i,j}^2 \end{cases}. \quad (11)$$

Then define NPCR as formula (12), which means the percentage of different pixels of two ciphertext images.

$$\text{NPCR} = \frac{\sum_{i=0}^{M-1} \sum_{j=0}^{N-1} D(i,j)}{M \times N} \times 100\%. \quad (12)$$

Furthermore, define UACI as formula (13), which means the average of the absolute difference of two ciphertext images.

$$\text{UACI} = \frac{\sum_{i=0}^{M-1} \sum_{j=0}^{N-1} |C_{i,j}^1 - C_{i,j}^2|}{255 \times M \times N} \times 100\%. \quad (13)$$

Table 7 shows encrypted Lena's NPCR and UACI at four specific positions, from which we can discover that the values are different at different positions. That is to say, these two indicators have randomness. For unity, let's reduce the first pixel at position (0,0) by 1, calculate the values of NPCR and UACI of six images based on formulas (12) and (13), list the numerical results in Table 8.

With a significance coefficient of 0.05, the ideal NPCR is 99.5693%, and UACI is 33.2824% for images of size 256×256 [51]. The results in Table 8 are all higher than the expected values, which proves that the algorithm in this article effectively passes the differential attack capability test. The comparison with other algorithms in case of Lena can refer to Table 5.

4.4. Robustness test

In the process of transmitting ciphertext images over the network, the data may be lost or attacked by noise, which requires the ciphertext image to have good anti-cutting and anti-noise attack performance. In other words, a good algorithm for image encryption should have robustness [52]. In addition, we can use PSNR to evaluate the quality of the decrypted image and the original image. The larger the value is, the more similar the two images, and the formula (14) is as follows:

$$\text{PSNR} = 10 \times \log_{10} \frac{M \times N \times 255^2}{\sum_{i=0}^{M-1} \sum_{j=0}^{N-1} (P(i,j) - C(i,j))^2}. \quad (14)$$

Taking Lena as an example, from the ciphertext image we respectively cut off 1/16, 1/8, 1/4 and 1/2 data at the top left corner, then decrypt the cut ciphertext images using the correct key. Fig. 9 displays the results, which clearly shows that even after its data is cut in half, the body of the image is still visible. The corresponding PSNR values of Fig. 9 are shown in Table 9. In summary, this algorithm indicates a good cutting resistance.

Table 5: Comparison with other algorithms

Image	Testing direction			Average value	Entropy	NPCR (%)	UACI (%)	Encryption time(s)	Decryption time(s)
	Horizontal	Vertical	Diagonal						
Ciphertext image in the proposed algorithm	-0.0006	-0.0036	-0.0016	0.0019	7.9978	99.617	33.5426	0.3077	0.2709
Ciphertext image in [4]	-0.0048	-0.0112	-0.0045	0.0068	7.9973	99.6228	33.7041	0.095	–
Ciphertext image in [34]	0.0179	0.022	7E-06	0.0133	7.9970	99.6107	33.4232	0.425	–
Ciphertext image in [35]	0.0018	0.0016	-0.0027	0.002	7.9974	99.6095	33.4649	0.2-0.23	0.13-0.17
Ciphertext image in [43]	0.000882	0.000108	0.000019	0.000336	7.9974	99.6102	33.3915	0.1062	–
Ciphertext image in [44]	-0.0226	0.0041	0.0368	0.02117	7.9963	99.6100	33.5300	0.613	–
Ciphertext image in [12]	0.0023	0.0158	0.0147	0.0583	–	99.6101	33.4583	0.325	–
Ciphertext image in [45]	-0.0059	-0.0146	0.0211	0.0139	7.9973	99.6100	33.4800	0.3243	–

Table 6: Information entropy of six ciphertext images

Image	Original image	Encrypted image
Lena	7.42489	7.99784
Baboo	7.37811	7.99737
Cameraman	7.03056	7.99748
Clock	6.70567	7.99775
Couple	7.05625	7.99723
Man	7.53608	7.99741

Table 7: Lena's NPCR and UACI at specific positions

Location	(209,232)	(33,234)	(162,26)	(72,140)
NPCR	0.996353	0.996185	0.996292	0.996246
UACI	0.334139	0.334155	0.33416	0.334107

Still taking Lena as an example, we respectively use salt and pepper noises with density 0.05, 0.1 and Gaussian noises with variance 0.01, 0.1 to attack. As shown in Fig. 10, the image is still visible, and the corresponding PSNR values of Fig. 10 are shown in Table 10, indicating a good performance to resist noise attacks.

4.5. Computational complexity and time efficiency

Any effective image encryption algorithm requires low computational complexity. In Algorithm 1, one chaotic sequence is generated with computational complexity $O(n)$, and three Latin squares are constructed with computational complexity $O(3n^2)$. In Algorithm 2, there is a three-layer encryption structure, which mainly uses an n -transversal for the first scrambling and Latin square for auxiliary diffusion and the second scrambling. The computational complexity is $O(n^3)$, so the

Table 8: The NPCR and UACI of six images

Image	NPCR	UACI
Lena	0.99617	0.335426
Baboo	0.996307	0.334622
Cameraman	0.996292	0.332594
Clock	0.996124	0.3351
Couple	0.996307	0.335925
Man	0.996078	0.333822

Table 9: PSNR with different cutting attacks

Image	PSNR values(dB)			
	cut 1/16	cut 1/8	cut 1/4	cut 1/2
Lena	18.4952	15.6102	12.7567	10.3489
Baboo	18.5505	15.5962	12.7419	10.4122
Cameraman	17.6986	14.8126	12.0811	9.6798
Clock	16.6901	13.6156	10.7295	8.1282
Couple	18.8945	15.8033	12.9758	10.5872
Man	17.7603	14.6126	11.7237	9.4005

Table 10: PSNR with different noises attack

Image	PSNR values(dB)			
	Salt & Pepper noise(0.05)	Salt & Pepper noise(0.1)	Gaussian noise(0.01)	Gaussian noise(0.1)
Lena	19.3543	16.5183	13.2037	11.9735
Baboo	19.3658	16.2732	13.1195	11.9209
Cameraman	18.4388	15.6301	12.2959	11.1939
Clock	17.4574	14.4200	11.0870	9.9733
Couple	19.4215	16.4731	13.0921	12.0530
Man	18.1337	15.3696	11.7741	10.7375

computational complexity of this algorithm is $O(n^3)$.

The fast encryption speed of the algorithm can meet the requirements of instant encryption. The experimental environment is MATLAB R2019b, Microsoft Windows 10 with Intel core i5-1135G7, 2.40 GHz processor and 16 GB RAM. Table 11 shows the encryption time and decryption time of six images, which are all calculated 20 times on average. It can be found that all encryption times approximately equal to 0.31s, decryption times approximately equal to 0.27s, and the comparison results of Lena and other algorithms are listed in the Table 5. It can be seen that the algorithm in this paper has relatively fast encryption speed.

Table 11: Encryption and decryption time of six images

Image	Encryption time	Decryption time
Lena	0.30769	0.27087
Baboo	0.30816	0.27063
Cameraman	0.30946	0.27259
Clock	0.30812	0.27233
Couple	0.30727	0.27219
Man	0.30769	0.27266

4.6. Resistance to classical types of attacks

There are four classical types of attacks: ciphertext only, known plaintext, chosen plaintext, chosen ciphertext. Among them, chosen plaintext attack is the most powerful attack. If an algorithm can resist this attack, it can resist others [3, 13].

The proposed algorithm only needs one round of encryption to achieve a safe effect. It depends on the plaintext image and is very sensitive to the initial parameters μ_0 and initial values key_0, key_1 . If the plain image or one key has changed, M, M_1, M_γ and D would be totally different. Further more, in the diffusion stage, encrypted value is not only related to plain value and former ciphered value, but also related to the second chaotic sequence and two Latin squares. So, the proposed algorithm can resist the chosen plaintext/ciphertext attack as well as other types of attacks.

5. Conclusion

In this article, a new chaotic algorithm for image encryption is proposed, mainly using transversals in a Latin square. An n -transversal can group all the positions and provide a pair of orthogonal Latin squares. So we can do scrambling in two ways, group by group and using the orthogonality of a pair of Latin squares, which obtains a nice scrambling effect. In the diffusion process, two suitable and uniform Latin squares are selected to do auxiliary diffusion based on a chaotic sequence, achieving good diffusion results. The proposed algorithm has successfully encrypted all test images, and passes the key sensitivity test, statistical test, plaintext sensitivity test, robustness test and other tests. Moreover, the entropy of each encrypted image is very close to 8, the correlation coefficient is very small, close to 0. From the above analysis, the algorithm in this article performs better than other contrast encryption algorithms. It shows that the algorithm achieves a secure and fast encryption effect, simultaneously has robustness and practicability.

Acknowledgments

The authors are grateful to Professor Jianguo Lei for some helpful discussions on the subject. This work was supported by National Natural Science Foundation of China [grant numbers 11871019, 11771119, 61703149]; and Foundation of Hebei Education Department of China [grant number QN2019127].

References

- [1] X. Liao, D. Xiao, Y. Chen, and T. Xiang, *Principles and applications of chaotic cryptography*. Beijing: Science Press, 2009.
- [2] J. Fridrich, "Symmetric ciphers based on two-dimensional chaotic maps," *International Journal of Bifurcation and Chaos*, vol. 8, no. 6, pp. 1259–1284, 1998.
- [3] X. Wang, L. Teng, and X. Qin, "A novel colour image encryption algorithm based on chaos," *Signal Processing*, vol. 92, no. 4, pp. 1101–1108, 2012.
- [4] A. Belazi, A. A. Abd El-Latif, and S. Belghith, "A novel image encryption scheme based on substitution-permutation network and chaos," *Signal Processing*, vol. 128, pp. 155–170, 2016.
- [5] E. Y. Xie, C. Li, S. Yu, and J. Lü, "On the cryptanalysis of Fridrich's chaotic image encryption scheme," *Signal Processing*, vol. 132, pp. 150–154, 2017.
- [6] X. Zhang and X. Wang, "Multiple-image encryption algorithm based on mixed image element and chaos," *Computers and Electrical Engineering*, vol. 62, pp. 401–413, 2017.
- [7] X. Wang, C. Liu, and D. Jiang, "A novel triple-image encryption and hiding algorithm based on chaos, compressive sensing and 3D DCT," *Information Sciences*, vol. 574, no. 1, pp. 506–527, 2021.
- [8] S. Li, G. Chen, and X. Mou, "On the dynamical degradation of digital piecewise linear chaotic maps," *International Journal of Bifurcation Chaos*, vol. 15, no. 10, pp. 3119–3151, 2005.
- [9] Z. Hua, F. Jin, B. Xu, and H. Huang, "2D Logistic-Sine-Coupling map for image encryption," *Signal Processing*, vol. 149, pp. 148–161, 2018.
- [10] Z. Hua, Y. Zhou, and H. Huang, "Cosine-transform-based chaotic system for image encryption," *Information Sciences*, vol. 480, pp. 403–419, 2019.
- [11] Z. Hua, Z. Zhu, Y. Chen, and Y. Li, "Color image encryption using orthogonal latin squares and a new 2D chaotic system," *Nonlinear Dynamics*, pp. 1–18, 2021.
- [12] X. Zhang, T. Wu, Y. Wang, L. Jiang, and Y. Niu, "A novel chaotic image encryption algorithm based on latin square and random shift," *Computational Intelligence and Neuroscience*, vol. 2021, pp. 1–13, 2021.
- [13] J. Zhou, N. Zhou, and L. Gong, "Fast color image encryption scheme based on 3D orthogonal latin squares and matching matrix," *Optics and Laser Technology*, vol. 131, p. 106437, 2020.
- [14] H. Liu and X. Wang, "Color image encryption based on one-time keys and robust chaotic maps," *Computers & Mathematics with Applications*, vol. 59, no. 10, pp. 3320–3327, 2010.
- [15] H. Liu and X. Wang, "Color image encryption using spatial bit-level permutation and high-dimension chaotic system," *Optics Communications*, vol. 284, no. 16–17, pp. 3895–3903, 2011.
- [16] Y. Zhou, W. Cao, and C. P. Chen, "Image encryption using binary bitplane," *Signal Processing*, vol. 100, pp. 197–207, jul 2014.
- [17] L. Xu, Z. Li, J. Li, and W. Hua, "A novel bit-level image encryption algorithm based on chaotic maps," *Optics and Lasers in Engineering*, vol. 78, pp. 17–25, 2016.
- [18] M. Xu and Z. Tian, "A novel image cipher based on 3D bit matrix and latin cubes," *Information Sciences*, vol. 478, pp. 1–14, 2019.
- [19] H. Liu, X. Wang, and A. Kadir, "Image encryption using DNA complementary rule and chaotic maps," *Applied Soft Computing*, vol. 12, no. 5, pp. 1457–1466, 2012.
- [20] X. Wang, Y. Zhang, and X. Bao, "A novel chaotic image encryption scheme using DNA sequence operations," *Optics and Lasers in Engineering*, vol. 73, pp. 53–61, 2015.
- [21] X. Chai, Y. Chen, and L. Broyde, "A novel chaos-based image

- encryption algorithm using DNA sequence operations,” *Optics and Lasers in Engineering*, vol. 88, pp. 197–213, 2017.
- [22] W. Dong, Q. Li, Y. Tang, M. Hu, and R. Zeng, “A robust and multi chaotic DNA image encryption with pixel-value pseudo-random substitution scheme,” *Optics Communications*, vol. 499, p. 127211, 2021.
- [23] A. H. Abdullah, R. Enayatifar, and M. Lee, “A hybrid genetic algorithm and chaotic function model for image encryption,” *AEU-International Journal of Electronics and Communications*, vol. 66, no. 10, pp. 806–816, 2012.
- [24] M. Zafari, S. Ahmadi-Kandjani, and R. Kheradmand, “Noise reduction in selective computational ghost imaging using genetic algorithm,” *Optics Communications*, vol. 387, pp. 182–187, 2017.
- [25] R. Premkumar and S. Anand, “Secured and compound 3-D chaos image encryption using hybrid mutation and crossover operator,” *Multimedia Tools and Applications*, vol. 78, no. 8, pp. 9577–9593, 2019.
- [26] Y. Zhang, Y. He, P. Li, and X. Wang, “A new color image encryption scheme based on 2DNLCML system and genetic operations,” *Optics and Lasers in Engineering*, vol. 128, p. 106040, 2020.
- [27] X. Wang and S. Gao, “Image encryption algorithm for synchronously updating Boolean networks based on matrix semi-tensor product theory,” *Information Sciences*, vol. 507, pp. 16–36, 2020.
- [28] X. Wang and S. Gao, “Image encryption algorithm based on the matrix semi-tensor product with a compound secret key produced by a Boolean network,” *Information Sciences*, vol. 539, pp. 195–214, 2020.
- [29] Y. Xian and X. Wang, “Fractal sorting matrix and its application on chaotic image encryption,” *Information Sciences*, vol. 547, pp. 1154–1169, 2021.
- [30] Q. Xu, K. Sun, C. Cao, and C. Zhu, “A fast image encryption algorithm based on compressive sensing and hyperchaotic map,” *Optics and Lasers in Engineering*, vol. 121, pp. 203–214, 2019.
- [31] J. S. Khan and S. K. Kayhan, “Chaos and compressive sensing based novel image encryption scheme,” *Journal of Information Security and Applications*, vol. 58, p. 102711, 2021.
- [32] Y. Wu, Y. Zhou, J. P. Noonan, and S. Agaian, “Design of image cipher using latin squares,” *Information Sciences*, vol. 264, pp. 317–339, 2014.
- [33] G. Hu, D. Xiao, Y. Zhang, and T. Xiang, “An efficient chaotic image cipher with dynamic lookup table driven bit-level permutation strategy,” *Nonlinear Dynamics*, vol. 87, no. 2, pp. 1359–1375, 2016.
- [34] M. Xu and Z. Tian, “A novel image encryption algorithm based on self-orthogonal Latin squares,” *Optik*, vol. 171, pp. 891–903, 2018.
- [35] X. Wang, Y. Su, M. Xu, H. Zhang, and Y. Zhang, “A new image encryption algorithm based on latin square matrix,” *Nonlinear Dynamics*, pp. 1–17, 2021.
- [36] G. Li, “A digital image scrambling method based on orthogonal Latin square,” *Journal of Northern University of Technology*, vol. 13, pp. 14–16, 2001.
- [37] J. Chen, Z. Zhu, C. Fu, L. Zhang, and Y. Zhang, “An efficient image encryption scheme using lookup table-based confusion and diffusion,” *Nonlinear Dynamics*, vol. 81, no. 3, pp. 1151–1166, 2015.
- [38] I. S. Sam, P. Devaraj, and R. Bhuvaneswaran, “An efficient quasigroup based image encryption using modified nonlinear chaotic maps,” *Sensing and Imaging*, vol. 15, no. 1, pp. 1–21, 2014.
- [39] C. E. Shannon, “Communication theory of secrecy systems,” *Bell System Technical Journal*, vol. 28, no. 4, pp. 656–715, 1949.
- [40] C. J. Colbourn, J. H. Dinitz, and D. R. Stinson, *Applications of combinatorial designs to communications, cryptography, and networking*. U. of Waterloo, Department of Combinatorics & Optimization, 1999.
- [41] A. B. Evans, *Orthogonal Latin squares based on groups*. Springer Science and Business Media LLC, 2018.
- [42] C. J. Colbourn and J. H. Dinitz, *Handbook of combinatorial designs 2nd ed.* Chapman and Hall/CRC, 2007.
- [43] H. Liu, B. Zhao, and L. Huang, “A novel quantum image encryption algorithm based on crossover operation and mutation operation,” *Multimedia Tools and Applications*, vol. 78, no. 14, pp. 20465–20483, 2019.
- [44] L. Xu, X. Gou, Z. Li, and J. Li, “A novel chaotic image encryption algorithm using block scrambling and dynamic index based diffusion,” *Optics and Lasers in Engineering*, vol. 91, pp. 41–52, apr 2017.
- [45] C. Cao, K. Sun, and W. Liu, “A novel bit-level image encryption algorithm based on 2D-LICM hyperchaotic map,” *Signal Processing*, vol. 143, pp. 122–133, 2018.
- [46] C. Jin and H. Liu, “A color image encryption scheme based on arnold scrambling and quantum chaotic,” *IJ Network Security*, vol. 19, no. 3, pp. 347–357, 2017.
- [47] A. Kulsoom, D. Xiao, S. A. Abbas *et al.*, “An efficient and noise resistive selective image encryption scheme for gray images based on chaotic maps and DNA complementary rules,” *Multimedia Tools and Applications*, vol. 75, no. 1, pp. 1–23, 2016.
- [48] K. A. K. Patro and B. Acharya, “Secure multi-level permutation operation based multiple colour image encryption,” *Journal of Information Security and Applications*, vol. 40, pp. 111–133, 2018.
- [49] S. Behnia, A. Akhshani, H. Mahmodi, and A. Akhavan, “A novel algorithm for image encryption based on mixture of chaotic maps,” *Chaos, Solitons & Fractals*, vol. 35, no. 2, pp. 408–419, 2008.
- [50] X. Sun, *Image encryption algorithm and practice-based on C sharp language implementation*. Beijing: Science Press, 2013.
- [51] Y. Wu, J. P. Noonan, S. Agaian *et al.*, “NPCR and UACI randomness tests for image encryption,” *Cyber Journals: Multi-disciplinary Journals in Science and Technology, Journal of Selected Areas in Telecommunications (JSAT)*, vol. 1, no. 2, pp. 31–38, 2011.
- [52] X. Wang and Z. Li, “A color image encryption algorithm based on Hopfield chaotic neural network,” *Optics and Lasers in Engineering*, vol. 115, pp. 107–118, 2019.

Appendix A. Proof of Theorem 2

Proof: 1) let $F = \{g_0, g_1, \dots, g_{n-1}\}$ be a finite field with character p . Cayley table M is a Latin square, the (i, j) th entry is $g_i + g_j$. By the definition of γ_j , it's easy to see that these γ_j s ($j = 0, 1, \dots, n - 1$) are n different bijections.

For any $x \in F$, define the mapping $\sigma_j : x \rightarrow x + \gamma_j(x)$, $j = 0, 1, \dots, n - 1$. Then

$$\sigma_j(x) = x + \gamma_j(x) = x + (ax + g_j) = (1 + a)x + g_j. \quad (\text{A.1})$$

Obviously, σ_j is bijective, then γ_j is a complete mapping of F under addition. By the definition of γ_j , these γ_j s are n different complete mappings of F .

2) By the definition of M_γ , it's easy to see that each element of F occurs exactly once in each row and column of M_γ . So M_γ is a Latin square too.

3) According to Theorem 1 and the definition of D , all columns of D form n disjoint transversals of M .

Firstly let's prove M_1 is orthogonal to M . By the definition of M_1 , the (i, j) th entry is $g_i + \gamma_j(g_i)$. That is

$$g_i + \gamma_j(g_i) = g_i + (ag_i + g_j) = (1 + a)g_i + g_j. \quad (\text{A.2})$$

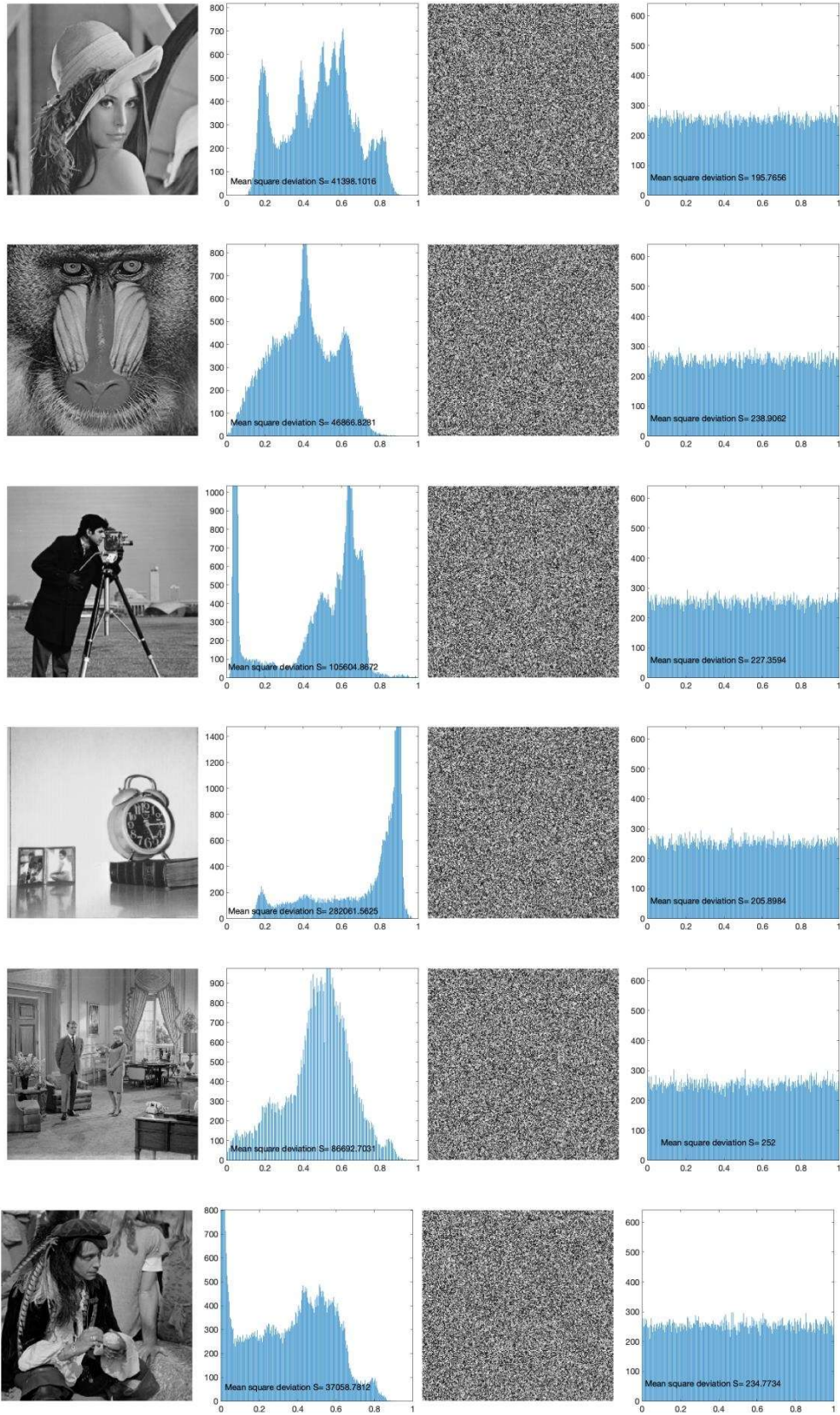
Because $a \neq 0, 1$ and $a \not\equiv -1 \pmod{p}$, M_1 is still a Latin square different from M, M_γ .

Assuming M_1 is not orthogonal to M , there must exist two positions $(i, j), (i', j')$, where $(i, j) \neq (i', j')$, such that $(g_i + g_j, (1 + a)g_i + g_j) = (g_{i'} + g_{j'}, (1 + a)g_{i'} + g_{j'})$, namely

$$\begin{cases} g_i + g_j = g_{i'} + g_{j'} \\ (1 + a)g_i + g_j = (1 + a)g_{i'} + g_{j'} \end{cases} \quad (\text{A.3})$$

Then either $(i, j) = (i', j')$ or $a \equiv -1 \pmod{p}$. Whatever either case, it's a contradiction with the definition of a or the assumption. Therefore M_1 is orthogonal to M .

Similarly, we can prove M_1 and M_γ , M and M_γ are pairwise orthogonal Latin squares. Theorem 2 is proved.



13
Figure 7: Histograms of six images: "Lena, Baboo, Cameraman, Clock, Couple, Man"

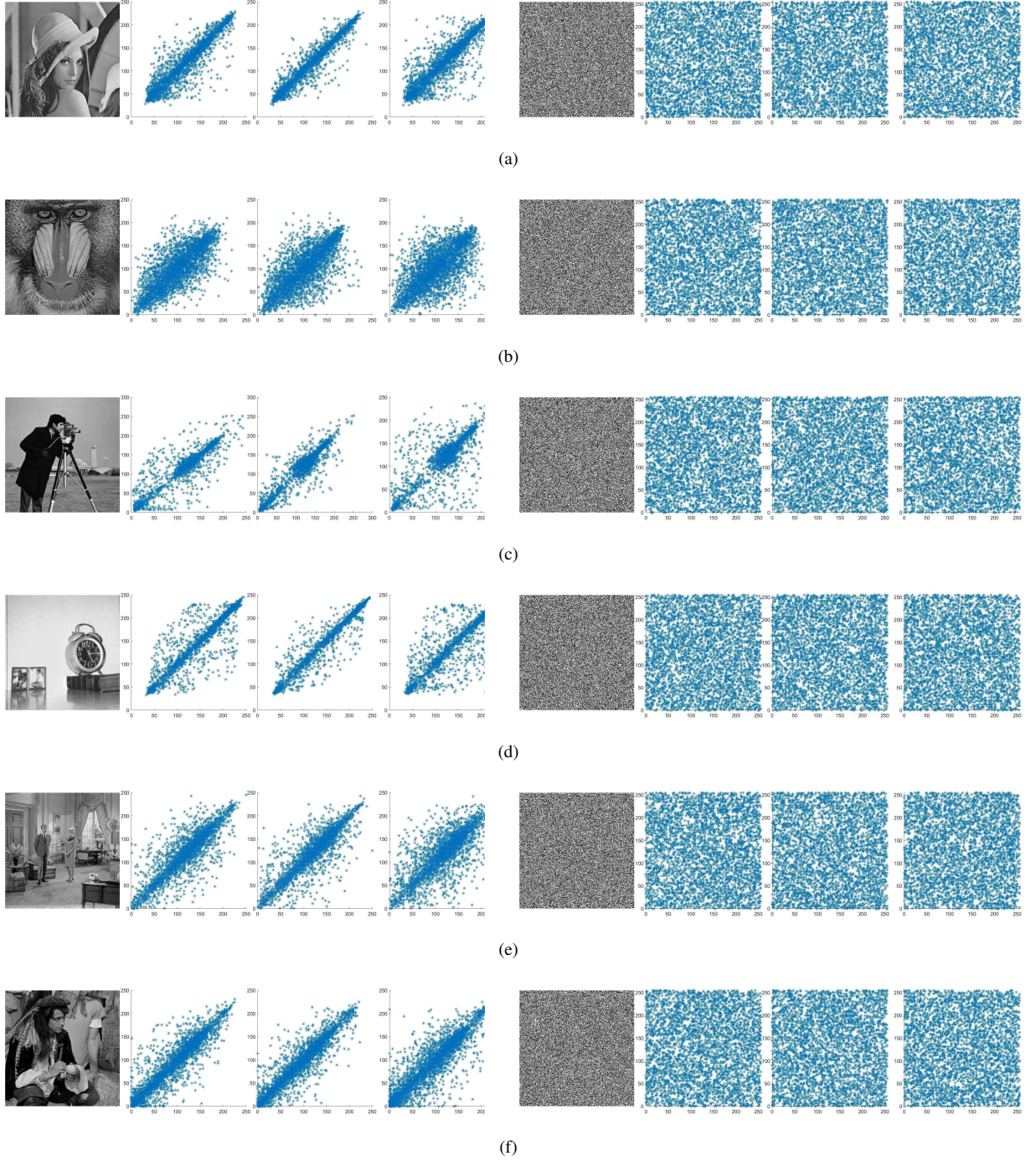
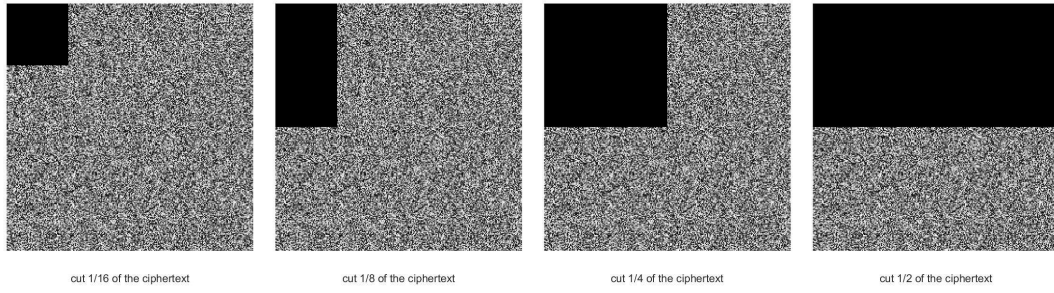


Figure 8: The correlation distribution of plaintext and ciphertext images in the horizontal, vertical and diagonal directions (from left to right) (a) Lena, (b) Baboo, (c) Cameraman, (d) Clock, (e) Couple, (f) Man

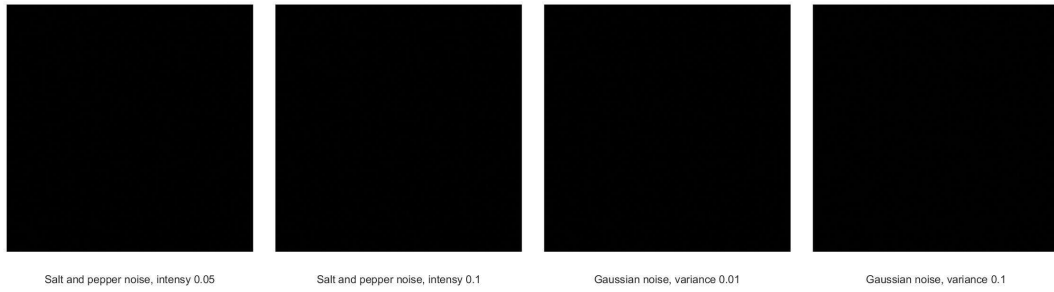


(a) Cut part of ciphertext

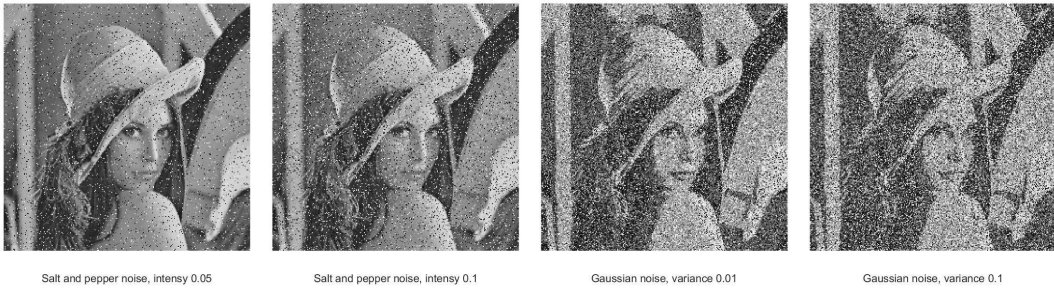


(b) Decryption of Fig.9(a)

Figure 9: Cutting attack resistance



(a) The encrypted image attacked by different types of noises



(b) Decryption of Fig.10(a)

Figure 10: Noise attack resistance